JOURNAL OF MATERIALS SCIENCE 32 (1997) 3943–3949

Fabrication and mechanical properties of fine-tungsten-dispersed alumina-based composites

TOHRU SEKINO, KOICHI NIIHARA
The Institute of Scientific and Industrial Research, Osaka University, 8-1 Mihogaoka, Ibaraki, Osaka 567, Japan

The mechanical properties and microstructure of fine-tungsten-dispersed alumina-based composites, which were fabricated by hot pressing a mixture of fine α-Al_2O_3 and W powders, have been investigated. Small W particles of approximately 140 nm average size were located within the Al_2O_3 matrix grains. The mechanical properties were influenced by the metal content and sintering conditions. When the appropriate W content and sintering condition were selected (typically 5–10 vol% W and sintered at 1400 °C), the fracture strength was enhanced compared with that of monolithic Al_2O_3. The metal content dependence of Young's modulus and the Vickers hardness did not obey the rule of mixtures. This may be attributed to the presence of localized residual stress caused by the incorporation of fine W dispersion into Al_2O_3. On the other hand, high-temperature (1600 °C) sintering caused degradation in the properties of the composites due to the grain growth and chemical reaction of W dispersion, which was revealed by X-ray photoelectron spectroscopy analysis. The relations between fabrication condition and mechanical properties are discussed.

1. Introduction

Recently many efforts to improve the mechanical and physical properties of ceramic materials have been made by controlling its nanostructure. Nanocomposites are nanostructured materials that have been widely investigated [1–11]. In these composites, nanometre-sized particles having a diameter from a few to several hundreds of nanometres are incorporated into glass or ceramic matrices [2]. Metal-particle-dispersed ceramic or glass nanocomposites have been studied from the view point of physical properties and/or electrical or optical applications [1–5]. Most of these systems were prepared by solution processes such as the sol–gel technique.

On the other hand, Niihara and co-workers [6–11] succeeded in developing dense ceramic–ceramic nanocomposites by a powder-metallurgical method in various oxide- and non-oxide-based composite systems [7–11]. The mechanical properties of these composites such as the fracture strength, toughness, thermal shock resistance and creep resistance were improved even at high temperatures. It follows that nanometre-sized metal particulate dispersion may also be used to improve the mechanical properties of ceramics.

Metal-particulate dispersions in ceramic materials have been previously studied, e.g., Al_2O_3 with the addition of W [12, 13], Mo [14, 15], Ni [16–18], Cr [19, 20] or Ti [21]. However, the enhancement of the mechanical properties of these composites was not sufficient to render them suitable for engineering applications.

On the basis of the results from the ceramic–ceramic nanocomposites [6–11], fine-metal-dispersed Al_2O_3-based composites have been developed in the Al_2O_3–W [22], Al_2O_3–Mo [23, 24] and Al_2O_3–Ni [25] systems to obtain ceramic–metal nanocomposites with desirable microstructures and much improved mechanical properties. Nawa *et al.* [23, 24] have demonstrated that the dispersion of a small amount of Mo in Al_2O_3 enhances the fracture strength whereas the addition of a large amount of metal results in toughening due to the crack-shielding effects by the elongated Mo phase. In the Al_2O_3–W system, however, the effects of the W volume fraction and the sintering condition on microstructures and mechanical properties have not been sufficiently clarified yet.

The purpose of the present work is to prepare high-density Al_2O_3–W composites with various metal contents by the usual powder-metallurgical method and to observe their microstructures. The relationships between the sintering conditions, microstructures and the mechanical properties (e.g., the fracture toughness, strength, hardness and elastic modulus) of the composites are discussed.

2. Experimental procedure

2.1. Fabrication

Commercially available high-purity α-Al_2O_3 powder (Sumitomo Chem. Co.; AKP-30; particle size, less than 0.3 μm) and W powder (Nippon Tungsten Co.; particle size, less than 0.4 μm) were selected as the raw

0022–2461

materials. No sintering additive was used in the fabrication. The starting mixed powders containing 2.5, 5, 7.5, 10 and 15 vol% W were obtained by the following procedure. Each raw material was mixed by the usual ball-milling technique with alumina balls in ethanol for 24 h. The mixtures were completely dried with a rotary evaporator at 60 °C for 2 h in vacuum and then dry ball milled for 24 h. During wet and dry milling, the pot was filled with Ar gas to minimize the oxidation of W powder. The mixtures were hot pressed at 1400–1600 °C under an applied pressure of 30 MPa for 1 h in Ar using a rectangular graphite die.

The sintered bodies, 30 mm × 40 mm × 5 mm in size, were cut with a diamond-blade saw, and the specimen surfaces were ground with a diamond wheel and polished with 9, 2 and 0.5 μm diamond pastes. The edges of the specimens were chamfered at 45°. The final dimensions of the specimen were 3 mm × 4 mm × 38 mm.

2.2. Characterization

The crystalline phases of composites were identified by X-ray diffraction analysis (XRD) (Rigaku RAD-C (Tokyo, Japan) instrument). The density of the specimens was measured by the Archimedes method in toluene. The microstructures were observed both by transmission electron microscopy (TEM) (Hitachi H-8100 electron microscope; 200 kV) and scanning electron microscopy (SEM) (Hitachi S-2150 electron microscope). TEM samples were prepared by cutting, grinding and polishing to form thin discs of 3 mm diameter and then thinned by Ar ion milling. Samples were coated with carbon to prevent the surface from charging up during TEM operation. The quantitative distribution of metal dispersion in the Al_2O_3–5 vol% W composite was estimated from the transmission electron micrographs using an image analysis technique. For the Al_2O_3–10 vol% W composites, X-ray photoelectron spectroscopy (XPS) (Shimadzu type-650B instrument) was employed using the Mg $K\alpha_{1,2}$ line ($h\nu = 1253.6$ eV) to analyse the oxidation state of dispersed W. Polished surfaces of the specimens were sputter cleaned by Ar^+-ion bombardment for 1 h inside the instrument before analysis. Young's modulus was determined by the resonance vibration method with the first-mode resonance. The fracture strength was measured by three-point bending at room temperature (span, 30 mm; cross-head speed, 0.5 mm min^{-1}). To determine the strength, six test pieces were used from each specimen. The fracture toughness was measured by the indentation fracture (IF) method [26] with a Vickers indentation using a load of 98 N and a loading duration of 15 s. Details of the fracture surface and the crack extension introduced by the Vickers indentation were observed by SEM. The hardness was also evaluated from the Vickers impression under the same condition as the IF test.

3. Results

3.1. Fabrication and microstructures

When γ-Al_2O_3 was used as a raw material, $AlWO_4$ and an unknown phase were detected by the XRD analysis, owing to the high reactivity of γ-Al_2O_3. As expected, the density of the specimen was low and the size of matrix grains was abnormally large, causing the specimen to be very fragile [24]. When α-Al_2O_3 was used as a raw material, on the other hand, the Al_2O_3–W composites were composed of only α-Al_2O_3 and W, and no byproduct was observed in the XRD analysis. In addition, a high density, above 98.5% of the theoretical value, was achieved for all composites. Thus, α-Al_2O_3 powder was finally selected as a raw material in this experiment.

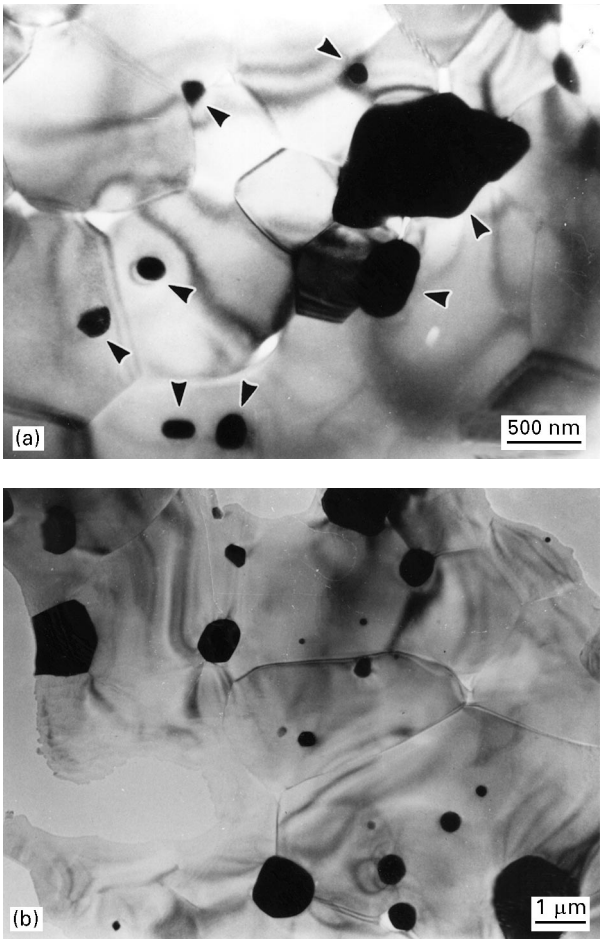

Figure 1 Transmission electron micrographs of the Al_2O_3–5 vol% W composite hot pressed at (a) 1400 °C and (b) 1600 °C. The arrows indicate W particles.

Fig. 1 shows the transmission electron micrographs of the Al_2O_3–5 vol% W composites hot pressed at 1400 and 1600 °C. In both composites, some pores were observed at triple-joint junctions of Al_2O_3 matrix grains or between matrix grains and dispersed W metal particles. The grain size of the Al_2O_3 matrix in the specimen hot pressed at 1400 °C (Fig. 1a) was fine, typically 1 μm. That of the composite sintered at 1600 °C was about 3–4 μm owing to grain growth. Under the same sintering condition, the matrix grain size of the Al_2O_3–W composites was smaller than that of monolithic Al_2O_3. This suggests that the presence of W dispersion inhibits the grain growth of the matrix.

From these micrographs, it is evident that the finer W particles were located both within the Al_2O_3

TABLE I The fraction and average particle size of the intragranular and intergranular W particles in the Al_2O_3–5 vol% W composite sintered at 1400 °C

	W particle dispersion		Al_2O_3 matrix
	Intragranular	Intergranular	
Number fraction (%)	16.6	83.4	—
Average particle size (nm)	137	340	960
	306[a]		

[a] Averaged particle size for all W dispersion in the composites.

matrix grains and at the grain boundaries, while the larger W particles over 1 μm in diameter were dispersed intergranularly in the Al_2O_3 matrix. In the case of the composite hot pressed at 1600 °C (Fig. 1b), the shape of large W dispersion is more spherical than that in the specimen hot pressed at 1400 °C, which is quite different from the elongated metal phase reported for the Al_2O_3–Mo system [24]. To clarify the microstructural characteristics, the particle size distribution of W in the Al_2O_3–5 vol% W composite sintered at 1400 °C was evaluated using the image analysis technique. The fraction and average particle size of the W in the composite body are summarized in Table I. It is noted that about 17% of the W particles were dispersed within the Al_2O_3 matrix grains with an average size of about 140 nm. The remaining 83% of W, which had an average size of about 340 nm, were located at the grain boundaries and/or the triple-point junctions of matrices.

3.2. The Vickers hardness and Young's modulus

The variation in the Vickers hardness with the W content is shown in Fig. 2. The broken and solid lines show the theoretical values calculated by assuming a linear relation between the hardnesses of Al_2O_3 (sintered at different temperature) and W. The hardness of the composites varied depending on the hot-pressing condition and the volume fraction of W. In the case of the specimens hot pressed at 1400 and 1500 °C, the variation in the Vickers hardness did not obey a linear relationship. At both temperatures, the hardness increased slightly with increasing W content up to 7.5 vol%. Above 10 vol% W, the value decreased with increasing W addition, as expected from the rule of mixtures. When the specimens were sintered at 1600 °C, the hardness values of the composites containing less than 10 vol% W were rather low, around 15 GPa.

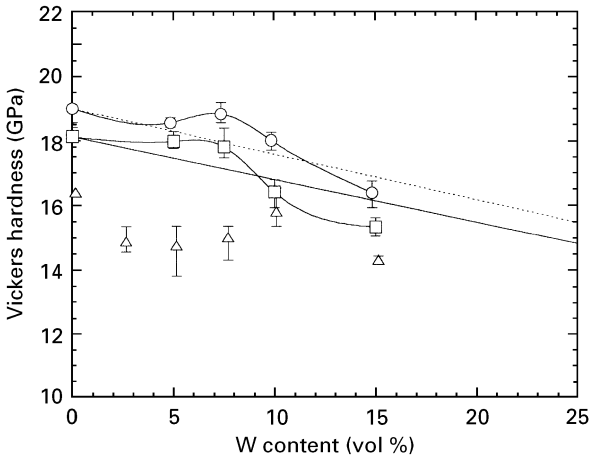

Figure 2 Variation in the Vickers hardness with the W content for the Al_2O_3–W composites. (○), 1400 °C; (□), 1500 °C; (△), 1600 °C. The broken and solid lines show the theoretical values calculated by assuming a linear relation of the hardness between Al_2O_3 and W. The hardnesses of Al_2O_3 used are 19.0 GPa and 18.1 GPa for the specimens sintered at 1400 °C (broken line), and 1500 °C (solid line), respectively. The hardness of W is 4.92 GPa (obtained from the high-purity W plate).

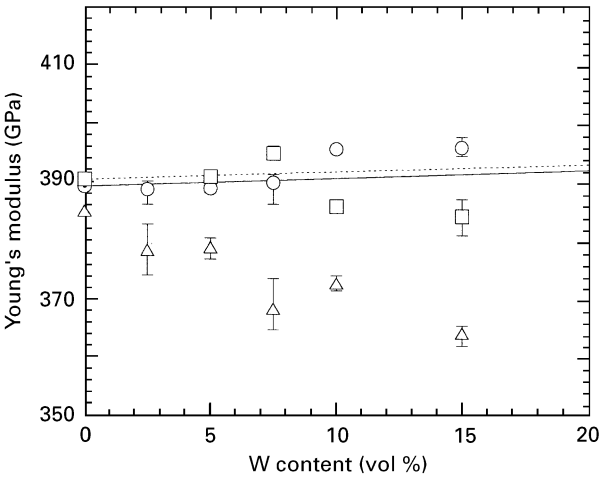

Figure 3 The dependence of Young's modulus on W content for the Al_2O_3–W composite. (○), 1400 °C; (□), 1500 °C; (△), 1600 °C. The solid and broken lines indicated are the theoretical value calculated by assuming the rule of mixture.

Fig. 3 shows Young's modulus of the Al_2O_3–W composites. The solid and broken lines in the figure are the calculated lines of the composites assuming the linear rule of mixtures. The values of Young's modulus for monolithic Al_2O_3 sintered at 1400 °C and 1500 °C were measured to be 389.3 GPa and 390.4 GPa, respectively. The modulus of the pure W metal was evaluated to be 404.7 GPa, which was in good agreement with the reported value of 410 GPa [27]. According to the rule of mixtures, it was predicted that Young's modulus of the composites might scarcely vary with the W content.

When the composite was hot pressed at 1400 °C, however, Young's modulus increased with increasing W content and reached a value of around 396 GPa at more than 10 vol% W. At 1500 °C, the maximum value appeared at 7.5 vol% W. On the other hand, much degradation was observed for composites hot pressed at 1600 °C, e.g., 364.3 GPa for Al_2O_3–15 vol% W.

3.3. Fracture strength

The fracture strengths of the Al_2O_3–W composites varied strongly depending on the hot-pressing conditions and the composition as shown in Fig. 4. For the hot pressing at 1400 °C, the strength increased with

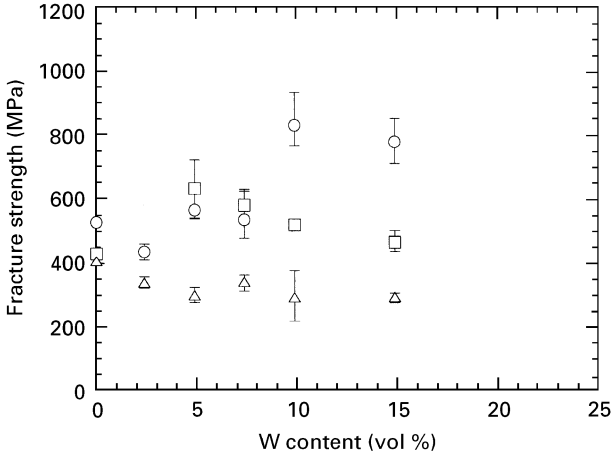

Figure 4 Variation in the fracture strength with the hot-pressing temperature and W volume fraction for the Al_2O_3–W composite (applied pressure for hot pressing, 30 MPa). (○), 1400 °C; (□), 1500 °C; (△), 1600 °C.

increasing W content and the maximum value of 831 MPa was observed at 10 vol% W. This maximum strength is about 60% higher than that of the monolithic Al_2O_3 (528 MPa) sintered at the same condition. On the other hand, no enhancement of strength was observed when the specimens were hot pressed at 1600 °C. The value of around 300 MPa was independent of the W content.

The fracture surfaces of the Al_2O_3–10 vol% W composites sintered at 1400 and 1600 °C are shown in Fig. 5. The fracture mode of the high-strength specimen, which has a fine matrix grain size, was both intergranular and transgranular as shown in Fig. 5a, while that of the low-strength material with large matrix grains exhibited mostly intergranular fracture.

3.4. Fracture toughness

Fig. 6 represents the variation in fracture toughness with the W content. In this figure, the toughness data for the Al_2O_3–15 vol% W hot pressed at 1600 °C was excluded because of the difficulty in getting a sufficiently smooth surface to estimate the toughness by the IF method. When the composites contained more than 7.5 vol% W and were sintered at 1400 and 1500 °C, their fracture toughness slightly increased compared with those of monolithic Al_2O_3. The highest toughness value (4.1 MPa $m^{1/2}$) was achieved for the Al_2O_3–10 vol% W specimen hot pressed at 1500 °C. When hot pressing was carried out at 1600 °C, however, the toughness decreased with increasing W content above 5 vol%.

A scanning electron micrograph of the indentation crack profile in the Al_2O_3–10 vol% W sintered at 1500 °C is presented in Fig. 7. As can be seen in this picture, the cracks mainly propagated through the Al_2O_3–W interfaces, and interlock bridging and/or pull-out were observed. Deformation of W particles such as necking was rarely confirmed in the present composites.

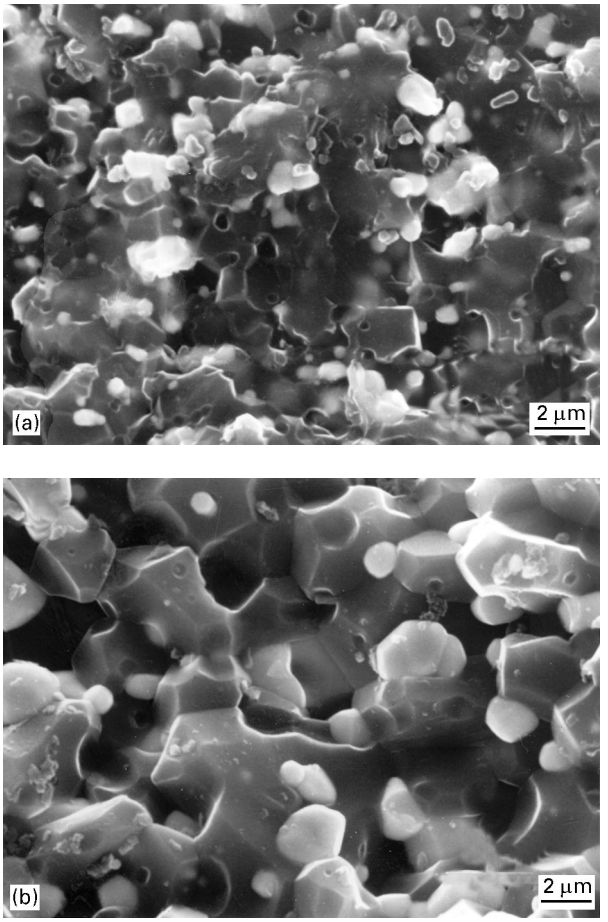

Figure 5 Scanning electron micrographs of the fracture surfaces for the Al_2O_3–10 vol % W composite hot pressed at (a) 1400 °C and (b) 1600 °C.

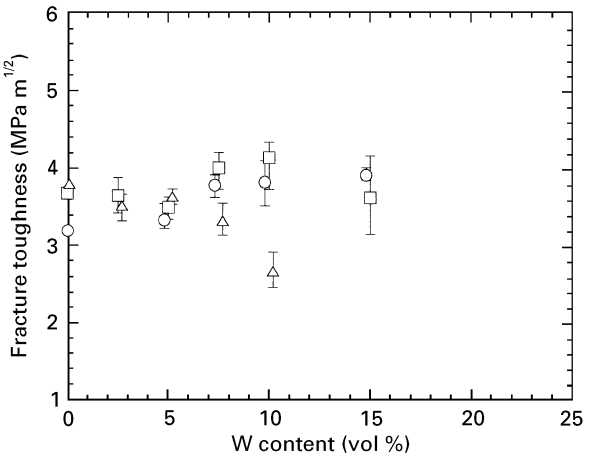

Figure 6 The dependence of fracture toughness on the W content and the hot-pressing temperature for the Al_2O_3–W composites. (○), 1400 °C; (□), 1500 °C; (△), 1600 °C.

4. Discussion

Microstructure observation for the Al_2O_3–5 vol% W composites revealed that the small W particles of approximately 140 nm average size were mainly located within the Al_2O_3 matrix grains. This suggests that fine-metallic-W-dispersed Al_2O_3 composite can be fabricated by a simple sintering technique. Large W particles are observed in the composites containing

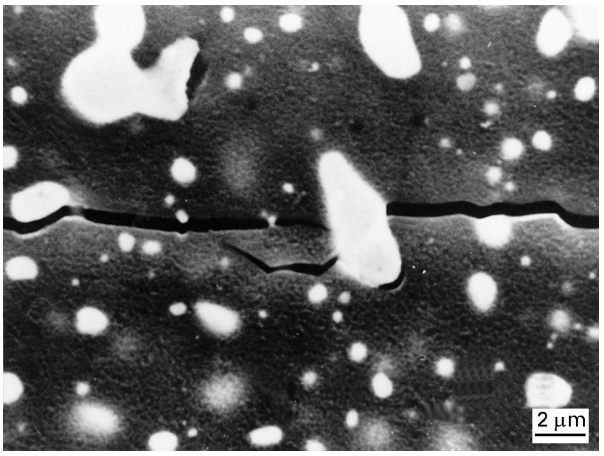

Figure 7 Scanning electron micrograph of the indentation crack on the surface of the Al_2O_3–10 vol% W composite hot pressed at 1500 °C.

much W dispersion and sintered at higher temperatures, which might be produced by the coalescence of W particles during sintering.

The mechanical properties of Al_2O_3 were influenced by the addition of fine W particles. The improvement of strength for the composites fabricated at 1400 °C can be mainly attributed to the decrease in grain size of the Al_2O_3 matrix. This reduces the size of flaws in the composites.

Another possibility for strengthening can be attributed to the presence of highly localized residual stresses generated from the thermal expansion mismatch between Al_2O_3 matrix and W dispersion. A similar strengthening mechanism is also observed for the Al_2O_3–SiC [6–10] and Al_2O_3–Mo [24] nanocomposites. For the Al_2O_3–W system, localized residual stresses around the W particulate dispersion can be calculated using the Selsing [28] model as follows:

$$\sigma = \frac{(\alpha_m - \alpha_p)\Delta T}{(1 + \nu_m)/2E_m + (1 - 2\nu_p)/E_p} \quad (1)$$

$$\sigma_r = -\sigma\left(\frac{r_0}{r}\right)^3 \quad (2)$$

where α, ν, E and ΔT are the thermal expansion coefficient, Poisson's ratio, Young's modulus and the temperature change during the cooling process, respectively. The subscripts m and p correspond to the values for the matrix and particle, respectively. σ_r indicates the component of vertical stress at ambient distance r from the centre of spherical enclosure. Therefore, σ_r at $r = r_0$ (radius of the particle) gives the maximum stress appearing at the matrix–particle interface.

In the present composites, σ_r $(r = r_0)$ is compressive with a calculated value of 1420 MPa when ΔT is assumed to be 1000 °C. As expected, XRD stress analysis by the iso-incrementation (fixed Φ angle) method (measured by the Rigaku RAD-R system) revealed that the compressive stress of 304 MPa for W dispersion was detected in the Al_2O_3–10 vol% W composite. The residual stress obtained was smaller than the calculated value because the stress might be relaxed by the plasticity during the cooling process. However, such internal stress appears to have a profound effect on the microfracture phenomena at the grain boundary and/or heterogeneous interface in the composites.

Mathematical and experimental studies on the polycrystalline brittle materials revealed that the microfracture of the grain boundaries was strongly affected by the localized residual stresses caused by the thermal expansion anisotropy of matrix grains [29, 30]. In the case of tensile stress perpendicular to the grain boundary, microcracking tends to occur at the interface, and the tensile stress at the grain boundary decreases the threshold stress for microcracking [30], thus causing the resultant strength of materials to decrease. Conversely, the existence of compressive stress at the grain boundary should strengthen the boundary. In the present composites containing a small amount of W and sintered at a low temperature, therefore, the interface strength might be increased by the presence of a large residual compressive stress, and this localized stress is expected to contribute to the enhanced strength of the composite when compared with the monolithic Al_2O_3.

Previous studies on ion implantation into an Al_2O_3 single crystal revealed the surface hardening of sapphire generated by low-dose implantation [31–33]. The increase in hardness was distinctly consistent with the compressive surface stress induced by the ion implantation. The morphologies of the second element in alumina are quite different for the implanted sapphire and the present composite. However, these would strongly suggest that the increment of hardness and Young's modulus beyond the expected value from the rule of mixtures for the present composites can be attributed to the internal stress originated from the thermal expansion mismatch between fine W and Al_2O_3 matrix.

On the other hand, the composites hot pressed at higher temperatures indicated poor mechanical properties. It was difficult to obtain a good milled surface by grinding and polishing for these composites. Chipping of matrix grains and intergranular fractures (Fig. 5b) were observed for the low-strength Al_2O_3–W composites. Obviously, this suggests that the Al_2O_3 matrix grain boundary or the interface between the matrix and the larger W particle is weak. For the Al_2O_3–Ti composites, reaction phases were observed at the Al_2O_3–Ti and Al_2O_3–Al_2O_3 interfaces and they played the role of a strong bonding phase [21]. On the contrary to the Al_2O_3–Ti composites, no byproducts were detected in the present composites by the XRD analysis. The present authors have focused on the XPS analysis of the composites which can detect a slight chemical reaction as a chemical shift in the binding energy.

The X-ray photoelectron spectra on the surface of WO_3 powder and Al_2O_3–10 vol% W sintered at various temperatures are shown in Fig. 8. Pure W metal which exhibits zero formal charge is reported to show two peaks of W $4f_{7/2}$ and $4f_{5/2}$ at 31.2 eV and 33.4 eV, respectively [34]. When tungsten is oxidized, the W4f

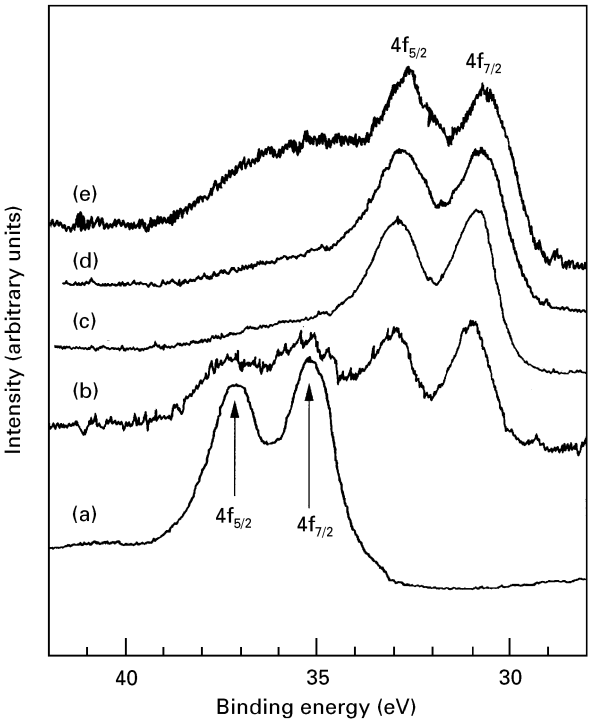

Figure 8 X-ray photoemission spectra of W 4f: (a) WO_3 powder; (b) Al_2O_3–10 vol% W hot pressed at 1400 °C, as polished; (c) Al_2O_3–10 vol% W hot pressed at 1400 °C, sputter cleared by Ar^+-ion bombardment for 1 h; (d) Al_2O_3–10 vol% W hot pressed at 1500 °C, sputter cleared by Ar^+-ion bombardment for 1 h; (e) Al_2O_3–10 vol% W hot pressed at 1600 °C, sputter cleaned by Ar^+-ion bombardment for 1 h.

peaks are well known to show a large chemical shift towards a higher binding energy. WO_3 powder exhibited two peaks at 35.0 eV and 37.6 eV (Fig. 8a), which are in good agreement with the reported values of 35.5 eV and 37.6 eV for $4f_{7/2}$ and $4f_{5/2}$, respectively [34].

In the case of as-sintered Al_2O_3–10 vol% W composite (Fig. 8b), four peaks were observed at 30.7, 32.8, 35.0 and 37.1 eV. The first two peaks can be attributed to W $4f_{7/2}$ and $4f_{5/2}$ with zero-formal-oxidation states which correspond to metallic W, and the last two peaks are found to exhibit W with +6 formal charge by comparison with WO_3 spectra. The existence of W^{6+} was easily confirmed by the surface oxidation of dispersed W due to grinding, polishing and handling in air. After Ar^+-ion etching, however, the 4f peaks corresponding to W^{6+} had disappeared, as shown in Fig. 8c. It is clear that the oxidation layer could be revealed by the Ar^+-ion bombardment.

The photoemission spectra of the etched Al_2O_3–10 vol% W composites fabricated at 1500 and 1600 °C also revealed the presence of W^0 peaks (Figs 8d and 8e). In the case of the specimen sintered at 1600 °C, a broad signal around 36 eV, which indicated the presence of W^{6+}, was observed (see Fig. 8e). It is not caused by the surface oxidation of W dispersion because the signal remained after long-time Ar^+ bombardment but probably originated from the intrinsic oxidation of W during the sintering process. Considering these facts (i.e., weak Al_2O_3–W interface and the presence of W^{6+}), it appears that a chemical reaction might have occurred at the Al_2O_3–W interface or at the matrix grain boundary by the hot pressing at higher temperatures.

The existence of large W particles as well as the coarse matrix grains, which were both caused by the progressive grain growth during sintering, are also compatible for the properties degradation. They introduce large initial flaws in the composites because of the weak interface between the W particles and Al_2O_3 matrices, hence reducing the composite strength. Much improved properties are, therefore, expected to be achieved if finer W particles are incorporated into Al_2O_3 matrix grains.

The toughness of Al_2O_3–W composites was clearly affected by the sintering temperatures (Fig. 6). A rather low fracture toughness was observed for the Al_2O_3–10 vol% W composite sintered at 1600 °C. As was discussed before, such composites are suspected to have weak interfaces which are considered to have a low localized fracture energy.

A slight increase in toughness was found for the composites sintered at 1400 and 1500 °C. Observed crack propagation phenomena were mainly related to the crack–microstructure interactions [35] such as interlock bridging and/or pulling out, which were often presented in micrometre-sized particulate dispersed composites. However, the toughening mechanism involving the plasticity of W or strong stress shielding effects by the dispersions which was reported for Mo-dispersed Al_2O_3 composite [24] was not predominant in the present system, owing to the spherical W particles.

5. Conclusions

Dense Al_2O_3–W composites were fabricated by the powder-metallurgical technique. W particles having an average diameter of about 140 nm were dispersed within the Al_2O_3 matrix grains. This indicates that the fine-W-particle-dispersed Al_2O_3 composite can be fabricated by the simple sintering technique. However, the larger W particles existed as a intergranular dispersion in the composites containing a large amount of W and hot pressed at higher temperature, owing to the coarse particles in the raw W powders and/or their grain growth during sintering.

The degradation of mechanical properties was observed when the composites were fabricated at higher temperatures. XPS observation revealed the existence of a small amount of W^{6+} in the specimen sintered at 1600 °C, which might result in the weakening of Al_2O_3–W or Al_2O_3–Al_2O_3 interfaces and poor mechanical properties such as the low strength and hardness of some composites.

The slight enhancement in toughness due to the interaction between the cracks and the large W particles was confirmed; however, the improvement is not predominant because of weak interface bonding and the morphological characteristics of the W dispersion. When the appropriate sintering condition and W content were selected, however, the mechanical properties of Al_2O_3, and in particular the fracture strength, were improved by dispersing a small amount of W and the resulting refinement of Al_2O_3 matrix grains. The

Vickers hardness and Young's modulus did not obey the rule of mixtures. This may be closely related to the presence of internal stress in the composites caused by the thermal expansion mismatch between the matrix and the metal dispersion.

Acknowledgements

The authors wish to thank Dr I. M. Low (Curtin University of Technology) and Dr A. Nakahira (Kyoto Institute of Technology) for their useful discussion. This research was supported by the Ministry of Education, Science and Culture under Grants-in-Aid for Scientific Research 01647001, 02205088 and 05750749.

References

1. R. A. ROY and R. ROY, *Mater. Res. Bull.* **19** (1984) 169.
2. R. ROY, *Science* **238** (1987) 1664.
3. A. CHATTERJEE and P. CHAKRAVORTY, *J. Phys. D: Appl. Phys.* **22** (1989) 1386.
4. R. D. SHALL, J. J. RITTER, A. J. SHAPIRO, L. J. SWARTZENDRUBER and L. H. BENNETT, *J. Appl. Phys.* **67** (1990) 4490.
5. A. CHATTERJEE and P. CHAKRAVORTY, *J. Phys. D: Appl. Phys.* **23** (1990) 1097.
6. K. NIIHARA, *Electron. Ceram.* **9** (1988) 44.
7. K. NIIHARA, A. NAKAHIRA, G. SASAKI and M. HIRABAYASHI, in "Composites, corrosion/coating of advanced materials", "Proceedings of the Fourth Materials Research Society International Meeting on Advanced Materials", Vol. 4, June 1988, Tokyo, edited by M. Doyama, S. Somiya and R. Chang, (Materials Research Society, PA, 1989) p. 129.
8. K. NIIHARA, T. HIRANO, A. NAKAHIRA, K. OJIMA, K. IZAKI and T. KAWAKAMI, in "Structural ceramics, fracture mechanics", "Proceedings of the Fifth Materials Research Society International Meeting on Advanced Materials", Vol. 5, June 1988, Tokyo, edited by M. Doyama, S. Somiya and R. Chang, (Materials Research Society, PA, 1989) p. 107.
9. K. NIIHARA, K. IZAKI and A. NAKAHIRA, *J. Jpn. Soc. Powder Powder Metall.* **37** (1990) 352.
10. K. NIIHARA, A. NAKAHIRA, H. UEDA and G. SASAKI, in "Proceedings of the First Japan SAMPE Symposium" Chiba, November 1989, edited by Z. Maekawa (SAMPE Japan, Tokyo, 1989) p. 1120.
11. K. NIIHARA, *J. Ceram. Soc. Jpn* **99** (1991) 974.
12. P. HING, *Sci. Ceram.* **10** (1980) 521.
13. *Idem., ibid.* **12** (1984) 87.
14. C. O. MCHUGH, T. J. WHALEN and M. HUMENIK Jr, *J. Amer. Ceram. Soc.* **49** (1966) 486.
15. D. T. RANKIN, J. J. STIGLICH, D. R. PETRAK and R. RUH, *ibid.* **54** (1971) 277.
16. E. BREVAL, G. DODDS and C. G. PANTANO, *Mater. Res. Bull.* **20** (1985) 1191.
17. W. H. TUAN and R. J. BROOK, *J. Eur. Ceram. Soc.* **10** (1992) 95.
18. E. ÜSTÜNDAG, R. SUBRAMANIAN, R. DIECKMANN and S. L. SASS, *Acta Metall. Mater.* **43** (1995) 383.
19. S. A. CHO, M. PUERTA, B. COLS and J. C. OHEP, *Powder Metall. Int.* **12** (1980) 192.
20. C. S. MORGAN, A. J. MOORHEAD and C. G. PANTANO, *Ceram. Bull.* **61** (1982) 974.
21. Y. NAERHEIM, *Powder Metall. Int.* **18** (1986) 158.
22. T. SEKINO, A. NAKAHIRA, M. NAWA and K. NIIHARA, *J. Jpn. Soc. Powder and Powder Metall.* **38** (1991) 326.
23. M. NAWA, T. SEKINO and K. NIIHARA, *ibid.* **39** (1992) 1104.
24. *Idem., J. Mater. Sci.* **29** (1994) 3185.
25. T. SEKINO, T. NAKAJIMA and K. NIIHARA, *Mater. Lett.* **29** (1996) 165.
26. K. NIIHARA, R. MORENA and D. P. H. HASSELMAN, *J. Mater. Sci. Lett.* **1** (1982) 13.
27. G. SIMMONS and H. WANG, in "Single crystal elastic constants and calculated aggregate properties" (MIT Press, Cambridge, MA, 2nd Edn, 1971) p. 290.
28. J. SELSING, *J. Amer. Ceram. Soc.* **44** (1961) 419.
29. A. G. EVANS, *Acta Metall.* **26** (1978) 1845.
30. Y. FU and A. G. EVANS, *ibid.* **33** (1985) 1515.
31. M. E. O'HERN, C. J. MCHARGUE, C. W. WHITE and G. C. FARLOW, *Nucl. Instrum. Methods B* **46** (1990) 171.
32. S. J. BULL and T. F. PAGE, *J. Mater. Sci.* **23** (1988) 4217.
33. R. NOWAK, K. UENO and M. KINOSHITA, in "Fracture mechanics of ceramics", Vol. 10, edited by R. C. Bradt (Plenum, New York, 1992) p. 155.
34. R. J. COLTON and J. W. RABALAIS, *Inorg. Chem.* **15** (1976) 236.
35. P. L. SWANSON, C. J. FAIRBANKS, B. R. LAWN, Y. W. MAI and B. J. HOCKEY, *J. Amer. Ceram. Soc.* **70** (1987) 279.

Received 9 August 1996
and accepted 20 January 1997